JACS
JOURNAL OF THE AMERICAN CHEMICAL SOCIETY

Article

pubs.acs.org/JACS

van der Waals Interactions Determine Selectivity in Catalysis by Metallic Gold

Juan Carlos F. Rodriguez-Reyes,[†,‡,⊥] Cassandra G. F. Siler,[‡] Wei Liu,[§] Alexandre Tkatchenko,[§] Cynthia M. Friend,*[,†,‡] and Robert J. Madix*[,‡]

[†]Department of Chemistry and Chemical Biology, and [‡]School of Engineering and Applied Sciences, Harvard University, 12 Oxford Street, Cambridge, Massachusetts 02138, United States

[⊥]Department of Industrial Chemical Engineering, Universidad de Ingeniería y Tecnología, Avenida Cascanueces 2221, Lima 43, Peru

[§]Fritz-Haber-Institut der Max-Planck-Gesellschaft, Faradayweg 4-6, D-14195, Berlin, Germany

Supporting Information

ABSTRACT: To achieve high selectivity for catalytic reactions between two or more reactants on a heterogeneous catalyst, the relative concentrations of the reactive intermediates on the surface must be optimized. If species compete for binding sites, their concentrations depend on their relative binding strengths to the surface. In this article we describe a general framework for predicting the relative stability of organic intermediates involved in oxygen-assisted reactions on metallic gold with broad relevance to catalysis by metals. Combining theory and experiment, we establish that van der Waals interactions between the reactive intermediates and the surface, although weak, determine relative stabilities and thereby dictate the conditions for optimum selectivity. The inclusion of these interactions is essential for predicting these trends. The concepts and methods employed here have broad applicability for determining the stability of intermediates on the surfaces of catalytic metals and specifically demonstrate the critical role of weak interactions in determining reaction selectivity among reactions of complex molecules.

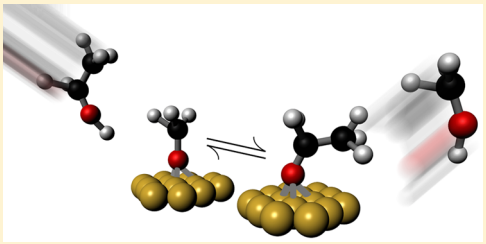

INTRODUCTION

Controlling reaction selectivity is key to achieving energy efficiency and conserving resources in heterogeneously catalyzed, sustainable chemical processes.[1] An important determinant of reaction selectivity in heterogeneous catalysis is the competition of reactants and intermediates for reaction sites,[2] which dictates the relative concentrations of species on the surface and, hence, the reaction selectivity and overall product yield.

A striking illustration of the importance of competitive binding of reactants for surface sites in detemining reaction selectivity arises in the oxidative cross-coupling of dissimilar alcohols over metallic gold, e.g., methanol and 1-butanol (Figure 1).[2] In this example the reactive intermediates are formed by reaction with adsorbed atomic oxygen (O_{ads}) to yield surface-bound alkoxy by transfer of the alcoholic proton to the adsorbed O_{ads}. Competition between the alcohols and the adsorbed alkoxy moieties determines the relative concentrations of the two alkoxides (Scheme 1) and the distribution of esters subsequently formed by bimolecular combinations of the alkoxy species.[2] Because the binding of 1-butoxy, the adsorbed intermediate derived from 1-butanol, dominates over methoxy with an equilibrium constant for the reaction in Scheme 1 being ~10, the optimum selectivity for the formation of methylbutyrate requires over 90% methanol in the reaction mixture in order to achieve a sufficient methoxy concentration (Figure 1).

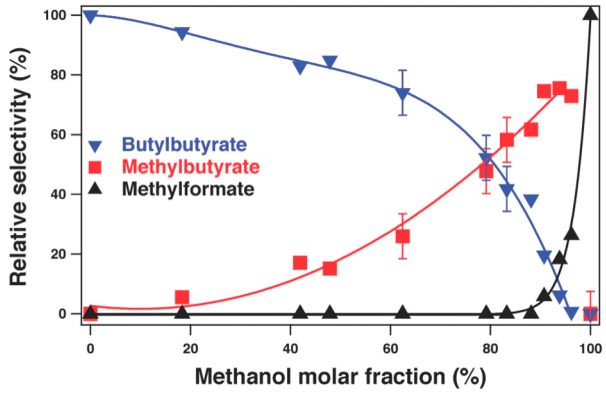

Figure 1. Selectivity for the esters formed from oxidative coupling of methanol and 1-butanol on O/Au(111) (θ_O = 0.1 ML) depends strongly on the CH_3OH:1-C_4H_9OH due to the competition for reactive sites on the surface. Reprinted from ref 2 with permission. Copyright 2010 American Chemical Society.

If the two alkoxides competed equally for binding sites, the optimum ratio of methanol to butanol would be 1:1.

Adsorbed intermediates that lead to side products, such as adsorbed carboxylates, also compete for binding sites, potentially affecting reactivity and selectivity.[3,4] The strength

Received: July 4, 2014
Published: August 29, 2014

   dx.doi.org/10.1021/ja506447y | J. Am. Chem. Soc. 2014, 136, 13333−13340

Scheme 1. Competitive Adsorption of Alcohols on a Catalyst Surface

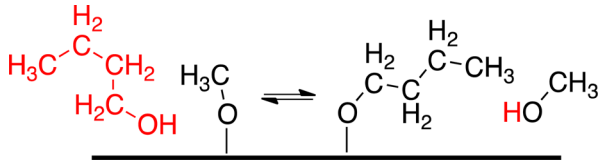

of their binding to the surface is thus important in determining catalytic activity as well as selectivity. Strongly bound species, such as carboxylates, may inhibit reaction by blocking formation of other key reactive intermediates.[5−7]

In this work we determine a hierarchy of stability with respect to displacement for a series of alkoxides and carboxylates on Au(111) as a first step toward understanding and predicting the competition for reactive sites and thereby controlling reaction selectivity. The underlying basis for our experimental studies is that organic acids and alcohols (generally designated as BH) selectively react with O bound to metallic gold[8] according to

$$2BH_{gas} + O_{ads} \rightarrow 2B_{ads} + H_2O_{ads} \quad (1)$$

On Au(111), the conjugate base, B_{ads}, can usually be isolated on the surface by heating the surface to 200 K to desorb the water, because below this temperature no further reactions occur. Most of the adsorbed intermediates studied here have been identified in previous studies[2,3,9−13] by a combination of vibrational and electronic spectroscopies and temperature-programmed reaction.

A hierarchy of stabilities of the intermediates B_{ads} is established here by investigating displacement reactions[12] on the metallic Au(111) surface,

$$B_{ads} + B'H_{gas} \leftrightarrows BH_{gas} + B'_{ads} \quad (2)$$

The displacement reactions establish a scale for the surface stabilities of intermediates key to oxygen-assisted coupling reactions on Au(111), B_{ads}, that serves as the basis for predicting the relative concentrations of adsorbed intermediates in reactive environments. Notably, reaction 2 relates to the relative stability of adsorbed B and B′ and does not require the presence of adsorbed O to proceed. Density functional theory (DFT) + van der Waals (vdW) was employed to a subset of these molecules to clarify the origin of the relative stabilities. The inclusion of the relatively weak vdW interactions is critical to predicting the order of stability of adsorbed oxygenates on Au(111). This paradigmatic approach has broad applicability to other classes of molecules on coinage metals (Cu, Ag, and Au) and to other metallic surfaces for predicting competition for binding sites that strongly affects catalytic activity and selectivity.

METHODS

Experimental Section. All experiments were performed under ultrahigh vacuum conditions in a chamber with a base pressure of ∼1 × 10^{-10} Torr. General procedures for crystal preparation and temperature-programmed reaction (TPRS) have been described previously[13,14] (see Supporting Information for details). The heating rate was constant at 5 K/s in all cases. Our experimental design included the collection of traces in the range m/z = 2 to m/z = 2m, where m is the molecular mass of the heaviest compound. Extensive calibrations and careful control of conditions were used to ensure that reproducible doses of the species were delivered to the surface (Figure S1, Supporting Information).

Experiments were generally performed on a Au(111) surface covered with 0.05 ML O. Atomic oxygen was generated by introducing ozone to the surface.[2,15] Ozone was produced using a commercial ozone generator (Ozone Engineering, LG-7) fed by an O_2 flow, generating a mixture of ∼10% O_3 in O_2, which was then introduced to the surface using a directed doser. The coverage of adsorbed O was calibrated by comparison of the integrated O_2 signal due to O atom recombination above 500 K to the integrated signal for the saturation coverage of 1.1 ML.[2,15]

Two types of experiments were performed to determine the relative adsorption strengths of different molecules −displacement reactions and competitive adsorption reactions. Common to both, the surface was first dosed with ozone to prepare a surface containing 0.05 ± 0.01 ML of adsorbed O, hereafter referred to as O/Au(111). For displacement reactions, a monolayer of BH was adsorbed on the 0.05 ML O/Au surface at 140 K, and the temperature was increased rapidly to a predetermined temperature to completely react the O_{ads} and desorb H_2O and excess molecular BH, isolating ∼0.1 ML B_{ads}. This method was used if only reaction 1 occurred below the predetermined temperature. Isolated B_{ads} was identified by subsequent cooling to 140 K and performing temperature-programmed reaction to ensure the absence of residual molecular species as well as to confirm the presense of B_{ads} by monitoring its reaction (for example, Figure S2, Supporting Information). The amount of residual adsorbed O following reaction this procedure was 0.0025 ML or less. After B_{ads} was isolated, an excess (0.5−1.0 ML) of a second species, B′H, was dosed at 140−200 K onto the surface to test the occurrence of reaction 2 above. The relative amounts of B_{ads} and B'_{ads} were distinguished by TPRS on the basis of the their signature products.

Alternatively, competitive adsorption was studied by dosing a mixture of BH and B′H onto the surface in excess of the preadsorbed 0.05 ML O/Au at ∼140 K (by dosing the equivalent of a full monolayer of BH and B′H combined). The relative stabilities of B_{ads} and B'_{ads} were judged by the competition of the two acids for the preadsorbed O, as determined by quantitative analysis of the product distribution measured subsequently by temperature-programmed reaction spectroscopy. This method was used when reactions of B_{ads} alone occurred at sufficiently low temperatures to preclude its isolation by annealing.

Theory. The calculations were carried out using the DFT + vdW^{surf} method,[16] which extends pairwise vdW approaches to modeling of adsorbates on surfaces by a synergetic combination of the DFT + vdW method[17] for intermolecular interactions with the Lifshitz−Zaremba−Kohn theory[18,19] for the nonlocal Coulomb screening within the bulk. Semilocal PBE functional[20] was used throughout the paper. We employed the "tight" settings for integration grids and standard numerical atom-centered orbitals basis sets in FHI-aims code.[21] We used the "tier2" basis set for light elements (such as H, C, O, and F) and "tier1" for Au. The atomic zeroth-order regular approximation (ZORA)[22] was used to treat relativistic effects for metal atoms. We utilized six-layer Au slabs with a (4 × 4) unit cell, and each slab was separated by a 40 Å vacuum. The bottom four metal layers were constrained, whereas the uppermost two metal layers and the adsorbate were allowed to fully relax during geometry relaxations. For slab calculations, we used a 3 × 3 × 1 k-points mesh.

RESULTS

The methodologies described above were used to determine the relative stability of specific intermediates (B_{ads}) utilizing their signature surface reactions. The species examined and the characteristic reaction products employed for the identification of B_{ads} are listed in (Table 1). The two methods described above are illustrated here with (1) the displacement of formate by trifluoroacetic acid and (2) the competitive reactions of coadsorbed formic acid and methanol with O/Au(111). These methodologies were used for other pairs of BH and B′H to

dx.doi.org/10.1021/ja506447y | J. Am. Chem. Soc. 2014, 136, 13333−13340

Table 1. Characteristic Reactions for Surface Species B_{ads} on Au(111), Which Are Derived from Organic Acids, BH

organic acid, BH (adsorbed conjugate base, B_{ads})	characteristic reaction products	peak temperature for products (K)
CF_3COOH (CF_3COO_{ads})	CO_2, CF_3	570
HCOOH ($HCOO_{ads}$)	CO_2	300
CH_3COOH (CH_3COO_{ads})	CO_2, CH_2CO	580
$CH_3(CH_2)_2COOH$ ($CH_3(CH_2)_2COO_{ads}$)	CO_2, CH_3CHCH_2	530
CF_3CH_2OH ($CF_3CH_2O_{ads}$)	$CF_3COOCH_2CF_3$	240
c-C_6H_5–CH_2OH (c-C_6H_5–CH_2O_{ads})	C_6H_5CHO	250
$CH_3(CH_2)_3OH$ ($CH_3(CH_2)_3O_{ads}$)	$C_3H_7COOC_4H_9$	300
CH_3CH_2OH ($CH_3CH_2O_{ads}$)	$CH_3COOCH_2CH_3$	220
HCCH (CCH_{ads})	HCCH	400
CH_3OH (CH_3O_{ads})	$HCOOCH_3$	220

establish the scale of relative stabilities for a broad range of adsorbed species; the data for which are in the Supporting Information.

Displacement of Formate by Trifluoroacetic Acid. The reaction pair of formic acid (HCOOH) and trifluoroacetic acid (CF_3COOH) exemplifies the displacement reaction; trifluoroacetate (CF_3COO_{ads}) is more strongly bound to the surface (Figure 2). By testing both orders of adsorption, we

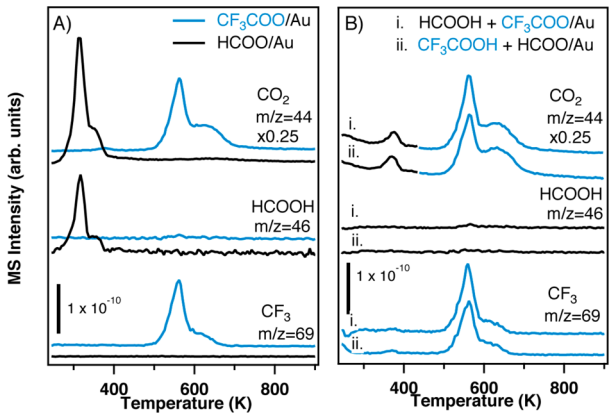

Figure 2. Displacement of formate by trifluoroacetic acid on Au(111) is demonstrated by monitoring characteristic decomposition reactions using a temperature-programmed reaction. (A) The characteristic "fingerprint" reaction products for reactions of the isolated formate (black) and trifluoroacetate (blue) yield different products and occur at very different temperatures. Formate decomposes to CO_2 and HCOOH at 300 K, whereas trifluoroacetate yields CO_2 and CF_3 at 580 K. (B) The exposure of adsorbed formate to excess trifluoroacetic acid yields products characteristic of adsorbed trifluoroacetate (at 580 K). The product amounts and temperatures are independent of the order of adsorption, clearly showing that trifluoroacetate binding is stronger.

demonstrate that thermodynamic, *not* kinetic factors, control the displacement process. The net reaction is

$$CF_3COOH_{ads} + HCOO_{ads} \rightleftarrows HCOOH + CF_3COO_{ads} \quad (3)$$

CF_3COO_{ads} was created by exposure of an excess of CF_3COOH to O/Au(111) (θ_O = 0.05 ML) at 140 K, followed by rapid heating to 400 K to desorb unreacted CF_3COOH and water in order to isolate CF_3COO_{ads}.

$$2CF_3COOH_{ads} + O_{ads} \rightarrow 2CF_3COO_{ads} + H_2O \quad (4)$$

The use of low surface concentrations of O guarantees the complete consumption of O during the reaction. Subsequent exposure of an excess of HCOOH at 200 K and heating showed only a minor amount of displacement of the trifluoroactate (Figure 2).

Similarly, formate was isolated by reaction of formic acid with adsorbed O:

$$2HCOOH_{ads} + O_{ads} \rightarrow 2HCOO_{ads} + H_2O \quad (5)$$

The adsorbed formate is displaced by exposure to excess CF_3COOH at 200 K (eq 3). The near complete displacement of $HCOO_{ads}$ by CF_3COOH was demonstrated by the absence of the *signature* products of formate decomposition (water and CO_2 at 280 K) and the presence of the *signature* products of CF_3COO_{ads} decomposition (CF_3 and CO_2 above 550 K) (Figure 2; Table 1). These data unequivocally demonstrate that CF_3COOH readily displaces $HCOO_{ads}$ from Au(111).

Further, the integrated intensities of the characteristic CF_3 and CO_2 signals above 550 K for CF_3COO_{ads} decomposition are the same to within experimental error (±20%) for pure CF_3COO_{ads} created from CF_3COOH reaction on O/Au(111), for exposure of the formate-covered surface to CF_3COOH, and for exposure of HCOOH to Au covered with the trifluoroacetate (all derived from 0.05 ML O/Au(111)). The small amount of CO_2 formed at 280 K is, however, indicative of a small amount of residual formate. Its presence does not affect any conclusions of this paper. On the basis of their relative gas phase acidities (eq 6, Table 2) CF_3COOH (1351 kJ/mol) is expected to displace $HCOO_{ads}$ to form trifluoro acetate and formic acid (1448 kJ/mol),[23] whereas the opposite reaction is not expected. The gas phase acidity is defined as the enthalpy of the gas phase reaction,

$$BH_{gas} \rightarrow B^-_{gas} + H^+_{gas} \qquad \Delta H_{acid} \quad (6)$$

Competitive Adsorption of Formic Acid and Methanol. The second method used to establish the relative stabilities of conjugate bases is coadsorption, which is illustrated here by the competition between methanol and formic acid for reaction with O/Au(111). This methodology was used to investigate intermediates that themselves react or decompose below 200 K, precluding their isolation by annealing. For example, methoxy forms from methanol on O/Au(111) and reacts to form methyl formate below 200 K, preventing the isolation of methoxy by annealing to temperatures sufficient to desorb water.

The signature of methoxy in temperature-programmed reaction is methyl formate (m/z 60), produced at 220 K,[10] whereas the fingerprint for formate is CO_2 production near 300 K (Figure 3). When methanol and formic acid are coadsorbed onto O/Au at 140 K, formate is formed exclusively, the dominant product being CO_2 near 300 K (Figure 3). The results of the competition of formic acid and methanol for adsorption on Au(111) is in accord with their respective gas phase acidities (1448 vs 1598 kJ/mol).[23]

$$CH_3O_{ads} + HCOOD \rightleftarrows CH_3OD + HCOO_{ads} \quad (7)$$

This experiment also shows that methoxy is *reversibly* formed on the surface in the displacement reaction, since CH_3OD is formed when CH_3OH and HCOOD are coadsorbed. This could occur by methoxy reaction with OD/D_2O (reactions 8–10), or methoxy directly reacting with HCOOD as in reaction 7

dx.doi.org/10.1021/ja506447y | J. Am. Chem. Soc. 2014, 136, 13333–13340

Table 2. Ordered Stabilities of Surface Intermediates, the Gas Phase Acidity and Bond Dissociation Energy of Their Parent Acid (BH), and the Reactions Used to Test Their Relative Stabilities[a]

Increasing surface stability

Conjugate Base	Gas Phase Acidity* (kJ/mol)	Bond Dissociation Energy† (kJ/mol)	Probe Reaction‡
Butanoate	1451 ±8	439.8	$1\text{-}CH_3(CH_2)_2COOH + CF_3COO_{(a)} \rightarrow 1\text{-}CH_3(CH_2)_2COO_{(a)} + CF_3COOH$
Trifluoro acetate	1351 ±12	452.3 ±12	$CF_3COOH + CH_3COO_{(a)} \rightarrow CF_3COO_{(a)} + CH_3COOH$
Acetate	1456 ±9	468.6 ±12	$CH_3COO_{(a)} + HCOOD \leftarrow CH_3COOD + HCOO_{(a)}$
Formate	1445 ±9	468.6 ±12	$C_6H_5OH + HCOO_{(a)} \rightleftharpoons C_6H_5O_{(a)} + HCOOH$
Benzyl alkoxy	1548 ±8	442.7 ±8.8	$C_6H_5OH + 1\text{-}CH_3(CH_2)_3O_{(a)} \rightarrow C_6H_5O_{(a)} + 1\text{-}CH_3(CH_2)_3OH$
Butoxy	1570 ±8	432.3	$1\text{-}CH_3(CH_2)_3OH + HCOO_{(a)} \leftarrow HCOOH + 1\text{-}CH_3(CH_2)_3O_{(a)}$
Ethoxy	1580 ±8	441 ±6	$1\text{-}CH_3(CH_2)_3OH + CH_3CH_2O_{(a)} \rightarrow 1\text{-}CH_3(CH_2)_3O_{(a)} + CH_3CH_2OH$
Trifluoro ethoxy	1513 ±10	447.7 ±10	$CF_3CH_2O_{(a)} + CH_3CH_2OH \rightarrow CH_3CH_2O_{(a)} + CF_3CH_2OH$
			$1\text{-}CH_3(CH_2)_3OH + CF_3CH_2O_{(a)} \rightarrow 1\text{-}CH_3(CH_2)_3O_{(a)} + CF_3CH_2OH$
Acetylide	1580 ±20	557.8 ±0.3	$HCC_{(a)} + CH_3OH \leftarrow HCCH + CH_3O_{(a)}$
Methoxy	1597 ±6	440.2 ±3	$CH_3CH_2OH + CH_3O_{(a)} \rightarrow CH_3CH_2O_{(a)} + CH_3OH$

[a]Lower values of gas phase acidity (ΔH) indicate stronger gas phase acids. *Gas phase acidity (taken from NIST database)[23] is defined as ΔH for $BH_{(g)} \rightarrow B_{(g)}^- + H_{(g)}^+$ (kJ/mol). Outliers to the gas phase acidity trend are indicated in bold. †The homolytic bond dissociation energy is defined as ΔH for $BH \rightarrow B_{(g)} + H_{(g)}$ (kJ/mol). The recommended values from the *Comprehensive Handbook of Chemical Bond Energies* are included here.[24] ‡The probe reactions are represented here as a dominant direction of equilibrium. Red arrows indicate a reversible but dominant direction. Black arrows indicate an irreversible reaction. As noted in the text, some probe reactions were displacement of an isolated intermediate, while others were competition experiments. The specific reaction data and conditions are provided in the Supporting Information (Section S.5, Figures S4–S12).

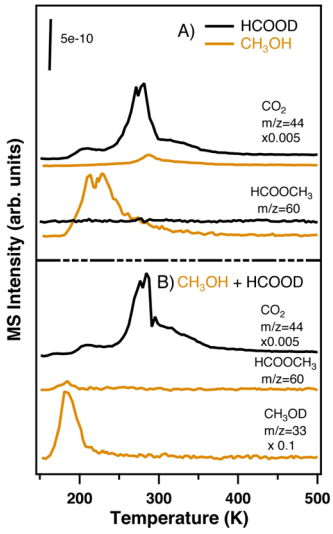

Figure 3. Temperature-programmed reaction demonstrates the predominance of formate binding to the surface when CH_3OH and HCOOH are coadsorbed on O/Au(111) (O = 0.05 ± 0.01 ML) at 140 K. (A) The characteristic reactions of formic acid (black) alone and pure methanol (gold). (B) The products observed from dosing a mixture of the two. Products characteristic of formate decomposition (CO_2) predominate in the mixture. Exposures were controlled to dose ~0.5 ML of each reactant.

$$CH_3OH_{ads} + O_{ads} \rightarrow CH_3O_{ads} + OH_{ads} \quad (8)$$

$$HCOOD_{ads} + O_{ads} \rightarrow HCOO_{ads} + OD_{ads} \quad (9)$$

$$CH_3O_{ads} + OD/D_2O_{ads} \leftrightarrows CH_3OD_{ads} + O/OD_{ads} \quad (10)$$

That gas phase acidities provide an overall guide to the displacement reactions was shown using acetylene and methanol competition. Their relative gas phase acidities predict that acetylene should dominate methanol in competition for binding sites on Au(111), whereas, for example, based on their C–H (~120 kcal/mol) and O–H (~100 kcal/mol) bond strengths[12] or their relative pK_a's, 26 and 15.5 respectively,[12] reaction 11

$$CH_3O + C_2H_2 \rightarrow CH_3OH + C_2H \quad (11)$$

is highly unfavored. Acetylene binds reversibly, without reaction, to Au(111), but in the absence of preadsorbed O, as for methanol, hydrogen abstraction and chemisorption is effected by O_{ads}. When acetylene and methanol were codosed onto 0.05 ML O/Au(111) at 140 K, reaction of acetylene *dominated* (Figure S3, Supporting Information). According to their relative gas phase acidities, reaction 12, this preference for adsorbed acetylide *is* reasonable,

$$CH_3O^-_{gas} + C_2H_{2gas} \rightarrow CH_3OH_{gas} + C_2H^-_{gas}$$

$$\Delta H = -17 \text{kcal/mol} \quad (12)$$

We thus conclude that the relative reactivity of these adsorbed intermediates on Au(111) can be correlated to their gas phase acidities and that the surface acetylide is, correspondingly, more stable than methoxy. This conclusion supports the hypothesis that the relative stabilities of the intermediates we have studied may be guided by the gas phase acidities of their parent molecules.

Reversible Displacement As a Probe of Competitive Binding. When the stability of two surface intermediates is similar, their relative surface concentrations can be varied by controlling the relative exposure of their precursor molecules

dx.doi.org/10.1021/ja506447y | J. Am. Chem. Soc. 2014, 136, 13333–13340

using reversible displacement. These experiments demonstrate that the relative concentrations of adsorbed reactive intermediates can be tuned by adjusting their relative concentrations in a reactant mixture, taking advantage of small differences in their surface stabilities. This effect is illustrated for acetic acid and formic acid (Figure 4), which compete for surface binding according to the equilibrium:

$$HCOOH_{ads} + CH_3COO_{ads} \leftrightarrows HCOO_{ads} + CH_3COOH_{ads} \quad (13)$$

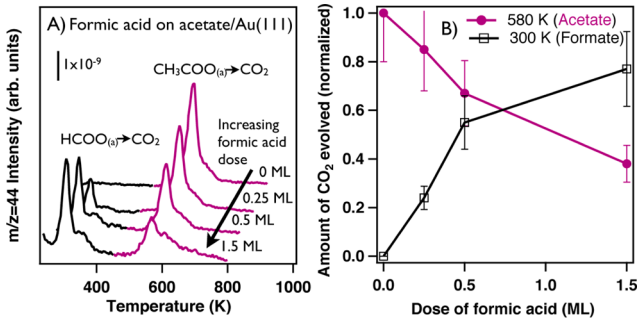

Figure 4. (A) CO_2 evolution from coadsorbed formate (300 K) and acetate (580 K) on Au(111) initially precovered with 0.1 ML acetate (CH_3COO_{ads}/Au) and exposed to 0.0−1.5 ML formic acid at 140 K. The acetate-covered surface was prepared by dosing excess acetic acid on 0.05 ML O/Au and annealing to 210 K to eliminate water and unreacted acetic acid. (B) The amounts of CO_2 evolved at 300 and 580 K are normalized to the amount of CO_2 for 0.1 ML of formate or acetate decomposition, respectively, found in separate experiments.

The total amount of $HCOO_{ads}$ and CH_3COO_{ads} is dictated by the amount of adsorbed O present prior to exposure to the mixture. Adsorbed acetate was formed initially by reaction of 0.05 ML O/Au(111) with acetic acid; it then was exposed to formic acid to form the mixed formate/acetate adsorbed layer. The amount of acetate remaining on the surface decreases with increasing formic acid exposure, based on the decrease in the amount of CO_2 produced from acetate decomposition (580 K) and the corresponding increase in the CO_2 yield due to formate decomposition (300 K) (Figure 4a). Within experimental control of the initial oxygen coverage (±0.01 ML), the sum of the formate and acetate coverage is constant. Acetate is never completely displaced by formic acid; ∼40% of the adsorbed acetate remains even for formic acid doses 15 times the acetate surface concentration (Figure 4b). This result indicates that surface bound acetate is more stable than formate.

Hierarchy of Binding. Overall, the stabilities of the surface intermediates studied increase as the gas phase acidities of their precursors (BH) increase, similar to previous studies on O/Ag(110).[12] Conversely, the relative stabilities do not correlate well with the homolytic bond dissociation energies (Table 2).[24,25] Since reaction 6 is the heterolytic bond cleavage of BH, the reaction is endothermic, and smaller values of $\Delta H_{(acid)}$ correspond to higher gas phase acidity. Further, H^+_{gas} is common to all such reactions, so the relative gas phase acidities scale directly with the electron affinity of B_{gas}. The fact that the gas phase acidities have been correlated with the polarizability of B for similar species suggest that weaker physical interactions of B_{ads} with the surface may play an important role in its stability.[26]

Relative gas phase acidities *strictly* employed would predict the equilibrium concentrations for the gas phase reaction

$$B^-_{gas} + B'H_{gas} \leftrightarrows BH_{gas} + B^{-\prime}{}_{gas} \quad (14)$$

Reactions 2 and 14 differ critically in that B^-_{gas} and $B^{-\prime}{}_{gas}$ are gas phase anions (reaction 14), whereas B_{ads} and B'_{ads} are bound to the surface (reaction 2). Thus, the heats of adsorption of B^-_{gas} and $B^{-\prime}{}_{gas}$ may, in some cases, be sufficiently different to alter the order of surface stability (and displacement) predicted by the gas phase acidities.

On O/Au(111) the stabilities progress from methoxy (ΔH_{acid} = 1597) to butanoate (ΔH_{acid} = 1451) in general agreement with the gas phase acidities of their parent acids (Table 2).[23] The reactions used to establish the comparative surface stabilities are listed in the right-hand column of Table 2. The data used for this table are summarized in the Supporting Information (Figures S4−S12). Notably, there are several exceptions to the trend with gas phase acidity, e.g., the fluorinated species, and formate vs acetate. The deviations from the correlation with the gas phase acidities require a more detailed examination of the surface bond energies of the intermediates using modern theoretical methods, as anticipated in the Introduction.

Calculations of Alkoxide Bonding. Calculations using the PBE + vdW^{surf} method were conducted to investigate the bonding of selected conjugate bases on the surface in order to provide more insight into the origin of the trends in binding energy. The structures and binding energies for a series of alkoxides bound to Au were examined: CH_3O_{ads}, $C_2H_5O_{ads}$, $CF_3CH_2O_{ads}$, and 1-$C_4H_9O_{ads}$. In all cases the structures and binding energies were calculated both with and without vdW interactions, since the widely used DFT functionals, including PBE used in the present work, fail to capture the long-range vdW interactions[27] (Table 3).

Table 3. Significant Effect of van der Waals (vdW) Interactions on the Binding Energies of Alkoxides on Au(111)

adsorbate	E_b (eV) PBE	E_b (eV) PBE + vdW	difference due to vdW (eV)
CH_3O	1.15	1.29	0.14
CF_3CH_2O	1.11	1.41	0.30
CH_3CH_2O	1.38	1.64	0.28
1-$CH_3(CH_2)_3O$	1.33	1.80	0.47

The trend in the bond strength of the various alkoxides to the Au(111) surface is accurately predicted *only* if vdW interactions are included (Table 3). For example, the bond energies of ethoxy ($CH_3CH_2O_{ads}$) and 1-butoxy (1-$C_4H_9O_{ads}$) are essentially the same when PBE functionals are used; however, the experiments show that 1-butoxy is more strongly bound (Table 2). When vdW interactions are included, both the absolute bond energies and the relative bond energies within this series are changed significantly (Table 3) such that CH_3Oads < $CF_3CH_2O_{ads}$ < $C_2H_5O_{ads}$ < 1-$C_4H_9O_{ads}$ as measured experimentally (Table 2). In contrast, calculations using the PBE functional alone predict that methoxy ≈ trifluorethoxy < ethoxy ≈ 1-butoxy; i.e. they do not reproduce experimental trends.

The increase in binding energies due to the inclusion of vdW interactions ranges from 0.14 eV for CH_3O_{ads} to 0.47 eV for 1-$C_4H_9O_{ads}$, accounting for ∼11% and ∼26% of the total binding energy, respectively. The contribution due to the long-range vdW interaction is ∼0.13 eV per carbon. Note that even though

dx.doi.org/10.1021/ja506447y | J. Am. Chem. Soc. 2014, 136, 13333−13340

the $CF_3CH_2O_{ads}$ is bound more weakly than the $CH_3CH_2O_{ads}$, the contribution due to van der Waals interactions is similar. The lower overall binding energy for the trifluoro-ethoxy is attributed to repulsion of the electron-rich CF_3 group and the surface leading to an overall lower binding energy. Note that the effect of this repulsion is also manifested even if van der Waals interactions are not included when PBE functionals alone were used (Table 3).

The vdW interactions also alter the structure of the adsorbed species as illustrated for the specific case of ethoxy bound to Au(111) (Figure 5). As might be anticipated, the inclusion of vdW interactions increases the Au−O−C1 bond angle from 123° to 134° such that the alkyl chain is tilted toward the surface. This tilting results in a decrease in the distance between the Au and C2 from 3.39 Å (PBE only) to 3.16 Å (PBE + vdW^{surf}), reflecting the attraction between the hydrocarbon tail and the Au surface. The distance between the Au surface and the O also increases by 0.06 Å when the vdw interactions are included for ethoxy. The elongation presumably reflects an optimization of the interactions between the Au and the O atom and the alkyl group. The relatively weak Au−O bond probably leads to the relatively large change in bond distance.

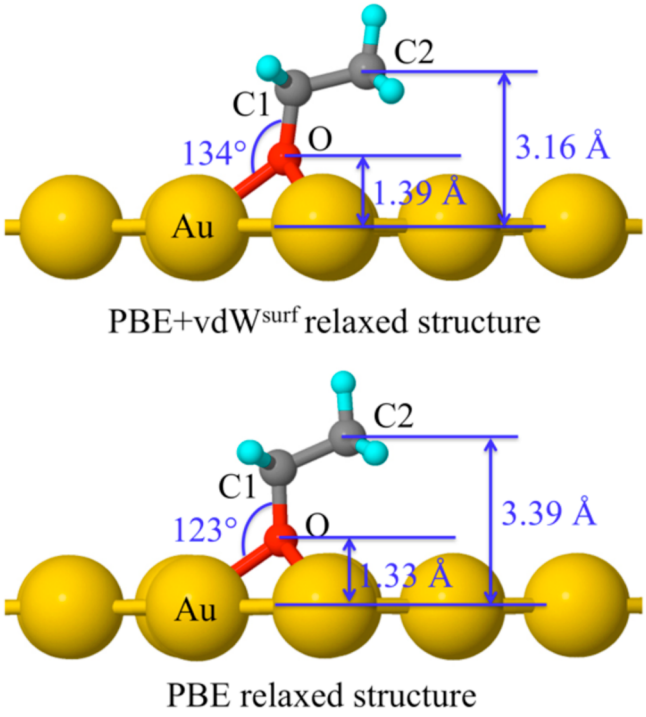

Figure 5. Structures of ethoxy (C_2H_5O) adsorbed on Au(111) with (top) and without (bottom) vdW interactions. Key bond lengths are changed by the vdW terms, including the Au−O, and Au−C2.

Similar structural changes occur when vdW interactions are included for the other alkoxides bound to Au(111) (Figures S13−S15, Supporting Information). The Au−O−C1 bond angle generally increases, and the distance between the terminal carbon and the surface generally decreases. Although the same trend is also observed for $CF_3CH_2O_{ads}$, the magnitude of the changes is smaller, probably due to repulsion between the electron-rich CF_3 group and the Au electrons. For example, the Au−O−C1 bond angle is smaller for $CF_3CH_2O_{ads}$ than for $CH_3CH_2O_{ads}$; the increase in this bond angle due to the inclusion of vdW interactions is also smaller—6° vs 11° for $CF_3CH_2O_{ads}$ vs $CH_3CH_2O_{ads}$. The change in the distance of O from the Au surface is also smaller for the trifluoro-ethoxy—0.04 Å compared to 0.06 Å for ethoxy, e.g., Figures 5 and S13−15. Note that the O−Au bond in the case of the $-CF_3$ group relative to the other alkoxides stems from the direct modification of the electronic structure and is fully reproduced by the PBE functional without including vdW interactions. All of these structural differences for the trifluoro-ethoxy reflect the balance between the attractive van der Waals and the Pauli repulsion for the interaction between the CF_3 group in the trifluoro-ethoxide.

DISCUSSION

In catalytic conditions, the hierarchy of relative stabilities can be used to guide adjustments in the partial pressures of reactants in order to achieve a desired ratio of concentrations of surface intermediates, thereby affecting desired product selectivity. Here we have focused on intermediates relevant to selective oxidative reactions on metals. For example, as noted in the Introduction, the selectivity for oxygen-assisted cross-esterification of different alcohols on gold can be controlled using this principle.[2] Alternatively, conditions may be designed to remove or mitigate unreactive spectator species that may inhibit reaction.

As suggested previously for metallic Ag surfaces, the adsorbed species under consideration can be classified as conjugate bases for gas phase H-acids, and the stability of these adsorbed conjugate bases with respect to displacement generally correlates with their gas phase acidities.[12] The advantage of this correlation is that gas phase acidities are accurately known for a wide range of molecules, therefore providing a simple parameter to predict trends in reactivity and competition for reactive sites. However, though the relative stabilities of these adsorbed conjugate bases of the O−H gas phase acids generally correlate well with the gas-phase acidities of the parent acid, BH (Table 2), the notable exceptions provoke deeper analysis of the stability trends.

The DFT + vdW calculations clearly demonstrate the need to include vdW interactions for correct description of the molecular surface bonding. In the homologous series of alkoxides, it is clear that weak interactions of the alkyl group significantly enhance the stability and the function of the adsorbed intermediates. For the C_1-C_4 linear alkoxides, both the gas phase acidities and the binding energies calculated by DFT + vdW predict the same trend in surface stability. This is perhaps not unexpected as the effect of alkyl groups on the gas phase acidity of a set of alcohols is attributed to stabilization of the negatively charged alkoxide through polarization of the alkyl group; thus, the polarizability correlates with gas phase acidity.[26] The strength of the vdW interactions also correlates with polarizability of the alkyl groups. It is clear from Table 3 that these interactions must be included to account for the experimental trends, and the theory provides key insight into the underlying reason for the correlations observed. Finally, it is notable that the binding energy trend calculated by PBE is modified and matches the experimental trend upon inclusion of the vdW interactions (Table 3).

There are notable exceptions to the correlation between conjugate base stabilities and gas phase acidities of the parent compounds, which are clarified by theory. Specifically, the relative stabilities of the fluorine-substituted adsorbed species, $CF_3CH_2O_{ads}$ and CF_3COO_{ads}, and of benzyl alkoxide, which contains a phenyl group, bound to Au(111) do not correlate

well with their gas-phase acidities. For example, though the gas phase acidity of CF_3CH_2OH is higher than ethanol, butanol, and benzyl alcohol, each of these species displaces $CF_3CH_2O_{ads}$, the reverse of the trend predicted by the gas phase acidities (Table 2). Likewise, trifluoroacetic acid (CF_3COOH) does not conform to the pattern predicted by its gas phase acidity (Table 2). Theory correctly accounts for these effects, showing that $CH_3CH_2O_{ads}$ is more strongly bound than $CF_3CH_2O_{ads}$, which in turn is more strongly bound than CH_3O_{ads}. Clearly this effect cannot be anticipated by the gas phase acidity correlation, since it does not account for differences in the heats of adsorption of the congugate bases of the gas phase acids. The weakened bonding due to fluorine substitution is found in calculations and is attributed to repulsion of the electron-rich CF_3 group from the Au (see Table 3). Such substituent effects result in the larger O−Au equilibrium distance for $CF_3CH_2O_{ads}$ than for $CH_3CH_2O_{ads}$ upon adsorption on the Au(111) surface (1.45 vs 1.39 Å), leading to a weaker chemical bonding for the $CF_3CH_2O_{ads}$/Au(111) system. The inclusion of vdW interactions is nevertheless important, increasing the binding energy of $CF_3CH_2O_{ads}$ by 0.30 eV, an amount slightly larger than that for $CH_3CH_2O_{ads}$ (0.28 eV). This is because the dispersion coefficient of F is somewhat larger than that of H (7.89 vs 2.42 Hatree Bohr).[28] We also note that the vdW interactions must be included in order to predict that the bonding of $CF_3CH_2O_{ads}$ is stronger than that of CH_3O_{ads}. The same conclusion was also found in the case of the $CF_3CH_2O_{ads}$ and 1-$CH_3(CH_2)_3O_{ads}$ pair (see Table 3).

The relative stabilities were also compared with the homolytic bond energies, and there is no obvious guideline from their relative values. For comparison the homolytic bond energies are listed in Table 2. Recent work on platinum[25] shows an elegant example of a correlation between surface bond strength and the homolytic B−H bond energy. Overall, the surface bond energies are approximately half the BH bond dissociation energy for a few select oxygenates on Pt(111). Though the results reported in that paper would predict that water would not spontaneously displace methoxy, as would be predicted on the basis of their gas phase acidities, application of the same scaling would **not** predict that acetylene would displace methoxy on gold. The binding energy of the acetylide to gold would have to be a substantially higher fraction of the bond dissociation energy of acetylene than was found for the correlation for the surface bond strengths of the oxygenates on Pt(111). In order to predict displacement from such information both the bond dissociation energy and the surface bond energy must be known (see SI). For the coinage metals, where dissociative adsorption of BH does not occur in the absence of adsorbed oxygen, these values may be hard to determine calorimetrically. Here we have shown that the displacements correlate well with the relative gas phase acidities, with understandable exceptions, as described.

Notably, the experimental trend in relative stability for carboxylates ($RCOO_{ads}$) is similar to the alkoxides:

$$HCOO_{ads} < CH_3COO_{ads} < CH_3(CH_2)_2COO_{ads}$$

The stability increases as a function of alkyl chain length. The gas phase acidity of the corresponding acids—formic, acetic, and 1-butanoic—are all quite similar (Table 1), suggesting that van der Waals interactions between the surface and the alkyl group affect the surface stability of the carboxylate. The carboxylates are more stable on the surface than the alkoxides investigated. This result is also in accord with the general observation that the carboxylates generally bind in a bidentate configuration to metal surfaces at low surface concentrations. The effect of the primary bonding interaction with the surface, of course, also affects the overall stability relative to other intermediates listed in Table 2. Future theoretical studies are required to address this point. Further, it can be shown that if the homolytic bond dissociation energy of the displacing molecule, B′H, exceeds that of the parent molecule of the species being displaced (BH, B_{ads}) (eq 2) the heat of adsorption of $B'_{(g)}$ is greater than that of $B_{(g)}$; i.e., B′ is more strongly bound (see SI). Thus, the data reveal that the carboxylate-Au interaction is stronger than the bonding of the alkoxides to the gold.

The other exception to the correlation between gas phase acidity and the stability of adsorbed conjugate base is benzyl alcohol (c-$C_6H_5CH_2OH$), which contains a phenyl ring that can interact with the surface. The gas phase acidity of benzyl alcohol lies between 1-butanol and formic acid (Table 2). Although it does displace 1-butanoate, consistent with the relative gas phase acidities, it is ***not*** displaced by formic acid. Instead, the stability of adsorbed formate and c-$C_6H_5CH_2O_{ads}$ is similar (Table 2, Figure S7, Supporting Information). On the basis of the calculations for the linear alkoxides (Table 3), we suggest that the higher stability of the benzyloxy (c-$C_6H_5CH_2O_{ads}$) compared to 1-butanoate is due to weak bonding interactions of the phenyl ring with the surface. Calculations are necessary to elucidate this point.

While the effect of van der Waals interactions is clearly important for predicting the binding strength of various intermediates to gold, it will be interesting to test for the magnitude of these effects on other surfaces. Generally, intermediates are bound relatively weakly to Au; thus the van der Waals interactions will naturally account for a larger percentage of the binding energy. In the case of 1-butoxide bound to Au(111), the van der Waals interaction accounts for ∼25% of the total bond energy (Table 3). On a per carbon basis the increase in binding energy of the linear alkoxides due to van der Waals interactions is ∼0.13 eV (∼3 kcal/mol). For a homologous series of adsorbed species, which may be involved in competitive catalytic reactions of similar reactants, these interactions may significantly affect relative surface concentrations because of the exponential dependence of the surface coverage on the heat of adsorption.

The demand and desire for reaction selectivity prediction has driven efforts to develop simple scaling relationships for rates of elementary surface reactions based on binding energies of specific atoms to metals surfaces using DFT studies.[29,30] While these scaling relationships have been relatively successful for predicting periodic trends in the bonding and reactivity of small molecules, e.g., diatomics, NH_3, CH_4, and CH_3O, they are less successful in predicting differences in binding for analogous species with different functional groups, e.g., binding of alkoxides (RO_{ads}) with alkyl groups with different chain lengths. These structural differences between molecules can be important in competitive binding of reactants in complex reaction environments[12,31] and are, therefore, important to understand.

It is very likely that the contributions of van der Waals interactions on the binding of intermediates such as the alkoxides will also be dependent on the metal surface, leading to periodic trends that will be superimposed on the scaling in the O-metal binding energy calculated using standard DFT methods. Additional experimental and theoretical studies are

necessary to establish these trends in the contribution of weak interactions to bonding to other surfaces so as to adjust scaling relationships for this critical factor. We also plan to further investigate similar trends in the binding of other functional groups to the surface in order to deepen our understanding of competitive binding in more complex reaction media.

CONCLUSIONS

A framework for predicting the relative stability of reaction intermediates important for selective oxidation on metallic gold has been developed from molecular gas phase acidities and DFT analysis including van der Waals interactions. The hierarchy was determined experimentally using displacement and competitive adsorption reactions of the parent molecules, and insight into the observed trends was provided by theory. The gas phase acidities of the parent molecules of these intermediates, BH, provide a general guide for the relative stability of the adsorbed intermediate, B_{ads}. Within that framework, however, notable exceptions arise, predominantly with molecules that have either significant surface binding energy increases due to vdW interactions or specific interactions due to other functional groups in the molecule. By including these interactions in the DFT calculations, the experimentally observed trend in these stabilities is understood. These conclusions and techniques provide a general approach toward predicting the relative stability of reaction intermediates on noble metal surfaces, which is crucial for the optimization of reaction selectivity in complex reaction environments.

ASSOCIATED CONTENT

Supporting Information

Experimental details for crystal preparation and temperature-programmed reaction spectra including control of reactant dosing, figure of the competitive adsorption of methanol and acetylene, the data for all experiments done to establish the stability hierarchy in Table 2, and figures detailing calculated structural changes for other alkoxys. Analyses for relationship of ΔH for dissociative adsorption to displacement, displacement to relative binding energies, and entropy for adsorbates are also included. This material is available free of charge via the Internet at http://pubs.acs.org.

AUTHOR INFORMATION

Corresponding Authors

cfriend@seas.harvard.edu
rmadix@seas.harvard.edu

Notes

The authors declare no competing financial interest.

ACKNOWLEDGMENTS

C.M.F. and C.G.F.S. gratefully acknowledge the support of the U.S. Department of Energy, Basic Energy Sciences, under Grant No. DE-FG02-84-ER13289 and the Graduate Fellowship Program (DOE SCGF), made possible in part by the American Recovery and Reinvestment Act of 2009, administered by ORISE-ORAU under contract no. DE-AC05-06OR23100. R.J.M. and J.C.R.R. acknowledge the support of the NSF under Grant CHE-0952790.

REFERENCES

(1) Bell, A. T.; Gates, B. C.; Ray, D. Basic research needs: Catalysis for energy. U.S. Department of Energy Report No. PNNL-17214, 2008, 1
(2) Xu, B.; Madix, R. J.; Friend, C. M. *J. Am. Chem. Soc.* **2010**, *132*, 16571.
(3) Liu, X.; Xu, B.; Haubrich, J.; Madix, R. J.; Friend, C. M. *J. Am. Chem. Soc.* **2009**, *131*, 5757.
(4) Barteau, M.; Bowker, M.; Madix, R. *J. Catal.* **1981**, *67*, 118.
(5) Hao, Y.; Mihaylov, M.; Ivanova, E.; Hadjiivanov, K.; Knözinger, H.; Gates, B. C. *J. Catal.* **2009**, *261*, 137.
(6) Schubert, M. M.; Venugopal, A.; Kahlich, M. J.; Plzak, V.; Behm, R. J. *J. Catal.* **2004**, *222*, 32.
(7) Daté, M.; Okumura, M.; Tsubota, S.; Haruta, M. *Angew. Chem., Int. Ed.* **2004**, *43*, 2129.
(8) Outka, D.; Madix, R. *J. Am. Chem. Soc.* **1987**, *109*, 1708.
(9) Xu, B.; Friend, C. M. *Farad. Discuss.* **2011**, *152*, 307.
(10) Xu, B.; Liu, X.; Haubrich, J.; Madix, R. J.; Friend, C. M. *Angew. Chem., Int. Ed.* **2009**, *48*, 4206.
(11) Cremer, T.; Siler, C.; Rodriguez-Reyes, J. C.; Friend, C. M.; Madix, R. J. *J. Phys. Chem. Lett.* **2014**, *5*, 1126.
(12) Barteau, M. A.; Madix, R. J. *Surf. Sci.* **1982**, *120*, 262.
(13) Rodríguez-Reyes, J. C. F.; Friend, C. M.; Madix, R. J. *Surf. Sci.* **2012**, *606*, 1129.
(14) Madix, R. J. *Surf. Sci.* **1994**, *299−300*, 785.
(15) Saliba, N.; Parker, D. H.; Koel, B. E. *Surf. Sci.* **1998**, *410*, 270.
(16) Ruiz, V. G.; Liu, W.; Zojer, E.; Scheffler, M.; Tkatchenko, A. *Phys. Rev. Lett.* **2012**, *108*, 146103.
(17) Tkatchenko, A.; Scheffler, M. *Phys. Rev. Lett.* **2009**, *102*, 073005.
(18) Lifshitz, E. M. *Sov. Phys. JETP* **1956**, *2*, 73.
(19) Zaremba, E.; Kohn, W. *Phys. Rev. B* **1976**, *13*, 2270.
(20) Perdew, J.; Burke, K.; Ernzerhof, M. *Phys. Rev. Lett.* **1996**, *77*, 3865.
(21) Blum, V.; Gehrke, R.; Hanke, F.; Havu, P.; Havu, V.; Ren, X.; Reuter, K.; Scheffler, M. *Comput. Phys. Commun.* **2009**, *180*, 2175.
(22) van Lenthe, E.; Baerends, E. J.; Snijders, J. G. *J. Chem. Phys.* **1994**, *101*, 9783.
(23) Mautner, M. *Ion Thermochemistry Data*; Linstrom, P. J.; Mallard, W. G., Eds.; National Institute of Standards and Technology: Gaithersburg, http://webbook.nist.gov, retrieved October 2013.
(24) Luo, Y.-R. *Comprehensive Handbook of Chemical Bond Energies*; CRC Press: Boca Raton, 2007.
(25) Karp, E. M.; Silbaugh, T. L.; Campbell, C. T. *J. Am. Chem. Soc.* **2014**, *136*, 4137.
(26) Brauman, J. I.; Blair, L. K. *J. Am. Chem. Soc.* **1970**, *92*, 5986.
(27) Tkatchenko, A.; Romaner, L.; Hofmann, O. T.; Zojer, E.; Ambrosch-Draxl, C.; Scheffler, M. *MRS Bull.* **2010**, *35*, 435.
(28) von Lilienfeld, O. A.; Tkatchenko, A. *J. Chem. Phys.* **2010**, *132*, 234109.
(29) Abild-Pedersen, F.; Greeley, J.; Studt, F.; Rossmeisl, J.; Munter, T. R.; Moses, P. G.; Skulason, E.; Bligaard, T.; Nørskov, J. K. *Phys. Rev. Lett.* **2007**, *99*, 016105.
(30) Nørskov, J. K.; Abild-Pedersen, F.; Studt, F.; Bligaard, T. *Proc. Natl. Acad. Sci. U. S. A.* **2011**, *108*, 937.
(31) Barteau, M.; Madix, R. *Surf. Sci.* **1982**, *115*, 355.